Chaperonin Point Mutation Enhances Cadmium Endurance in *Saccharomyces Cerevisiae*

Ankita Dube
National Institute of Technology Calicut
M Anaul Kabir (anaulk@nitc.ac.in)
National Institute of Technology Calicut School of Biotechnology https://orcid.org/0000-0003-0042-7795

Research Article

Keywords: TriC/CCT, protein aggregation, cadmium, vacuole sequestration, YCF1, BPT1.

Posted Date: April 26th, 2021

DOI: https://doi.org/10.21203/rs.3.rs-382413/v1

Abstract

Objective:

To study the effect of the mutation in conserved G412E in Cct7p subunit of CCT complex on its cellular fate.

Results:

TriC/CCT is a dynamic multimeric protein that assists in protein folding in energy-dependent manner. A point mutation in the ATP binding pocket in the equatorial domain of Cct7p subunit causes a delay in doubling time. The cell's size was twice the wild type, and the formation of protein aggregates suggests disturbed folding of the proteins. Upon growing in stressful conditions of arsenous acid and cadmium chloride, mutant was found to be lethal in As^{3+} but grew well in Cd^{2+} with 10.59µg cadmium uptake mg^{-1} compared to wild type. The increased expression of vacuole transporters *YCF1* and *BPT1* by ten-fold and two-fold in mutant indicates the metal transportation to the vacuole.

Conclusion:

CCT complex was vulnerable to the mutation in G412E in Cct7p subunit of protein folding molecular machinery. Interestingly, already stressed cells provided robustness against oxidative stress and cadmium sequestration in the vacuole.

1. Introduction

Chaperones are required for proper folding of the nascent polypeptide synthesis ensue in the lumen of the cell. These chaperones bind non-covalently with the exposed hydrophobic surfaces of newly formed polypeptides to prevent them from misfolding. Molecular chaperones are essentially not an element of the final form of a protein. The chaperonin TriC/CCT complex is involved in folding approximately 10% of cellular proteins, including cytoskeleton protein actin and tubulin (Thulasiraman et al. 1999; Yam et al. 2008). The CCT complex is composed of 16 subunits encoded by eight paralogous essential genes *CCT1-8*. The arrangement of subunits is in a ring-shaped manner containing eight related but different subunits. Two such rings are stacked upon each other to assemble into a cylindrical structure with a central cavity. This cavity provides a secluded environment for native protein to fold into its three-dimensional functional form. Each subunit comprises of three domains- apical, intermediate, and equatorial. The apical domain interacts with the substrate to be folded by the complex and contains a helical extension that forms the lid. It has open and close forms that enable the folding of the substrate by binding and hydrolysis of ATP in the equatorial domain. Intermediate domain coordinates between these two domains (Gestaut et al. 2019; Spiess et al. 2004). Each subunit has a distinct affinity to ATP, and hydrolysis occurs sequentially, aiding in diverse substrate folding. Amongst these eight subunits, five

subunits, such as Cct4p, Cct5p, Cct2p, Cct1p, and Cct7p, have higher affinity than subunits Cct3p, Cct6p, and Cct8p and arranged into two asymmetrical planes of high and low-affinity subunits (Amit et al. 2010; Reissmann et al. 2012).

Loss of function mutation in any of the subunits often disturbs protein folding. Mis-folded proteins have exposed hydrophobic moiety that may form aggregates with other polypeptides present in overly crowded cytosol. In neurodegenerative disorders like Alzheimer's (AD) and Huntington's (HD) diseases, cellular protein aggregation occurs in neurons. A mutation altering aspartate to glutamate in the P-loop of ATP binding pocket in Cct3p leads to loss of interaction with Q/N rich protein aggregates (Carmichael et al. 2000; Nadler-Holly et al. 2012). Oxidative stress and protein aggregates are indicators of neurodegenerative disorders. Oxidative stress causes oxidative peroxidation of unsaturated fatty acids and produces 4-hydroxy-2, 3-neonenal (HNE). In Alzheimer's disease, levels of HNE in plasma are high (Selley et al. 2002). A decline in glutathione levels was seen in Parkinson's disease and determined as a potential biomarker in the disorder's progression (Mischley et al. 2016). The yeast *Saccharomyces cerevisiae* is a well-established eukaryotic model system with a defined genetic system and eases to carry out genetic manipulation. It has been extensively used to understand many human diseases due to the similarity of core biological processes. For example, the expression of alpha-synuclein A53T mutant induces abnormal folding of HD proteins in yeast models, leads to the discovery of CCTs ability to alleviate the phenotype (Sot et al. 2017).

The GGG (412–414 in Cct7p) motif of ATP binding pocket in the equatorial domain is conserved from bacterial counterpart GroEL to human CCT. Moreover, the motif is conserved amongst the eight subunits of yeast except in Cct6p and Cct8p, in which GAG sequence is present instead of GGG. As the GGG motif occurs in the equatorial domain, it is predicted to have a role in ADP binding (unpublished docking data) (Chagoyen et al. 2014). The subunits Cct6p and Cct8p remain ADP-bound and do not participate in the ATPase cycle of the complex (Jin et al. 2019). Mutation in the GGG motif of Cct1p leads to temperature sensitive phenotype, whereas the same mutation in Cct6p does not affect its growth (Lin et al. 1997; Ursic et al. 1994). Herein, we have created a point mutation by modifying glycine to aspartic acid at 412 position (G412D) of the amino acid sequence in Cct7p to study the role of the conserved motif GGG (412–414) of ATP binding pocket. The mutation caused growth defects, altered cell morphology, and protein accumulation. We have also observed a possible cross-talk between aggregation and oxidative stress pathways.

2. Materials And Methods

2.1 Media and growth condition

Escherichia coli strain XL1-Blue was routinely grown at 37^0C in YT medium (0.5% yeast extract, 1% tryptone, 0.5% sodium chloride). 100µg Ampicillin ml^{-1} was added for isolation of the plasmid. YPD (1% yeast extract, 2% peptone, 2% dextrose) and SD (synthetic dextrose) media were prepared as described. 5-Fluoro orotic acid (5-FOA), an analog of uracil, was used to evict the plasmid containing the *URA3* gene.

For FOA plate preparation, 1 mg 5'-FOA ml^{-1} was added after autoclaving the media. YPD was used for growth assay, and 1mM arsenous acid, 1mM sodium arsenate, 2mM copper sulphate, 2mM zinc sulphate, 1mM cadmium chloride and 1% lactic acid were added wherever required. The spot assay was done on the solid medium by applying dilutions of 10^4, 10^3, 10^2, and 10^1 colony forming unit (CFU) per spot.

2.2 Vectors, plasmid constructions and primers

The yeast vectors pRS315, pRS316 and pRS11326 were used for maintaining constructs and assessing the phenotypes. The plasmid pUC19 was used for deletion construct. The *CCT7* gene (2153 bp) was amplified by PCR using primers KC124 and KC125 cloned into pJET1.2/blunt cloning vector. Subsequently, it was sub-cloned into pRS316 at BamHI-SalI site generating the plasmid pKA376. Upstream (591 bp) and downstream (506 bp) sequences of *CCT7* were amplified using the primers KC126/KC127 and KC128/KC129. The PCR amplified products were cloned into vector pTZ57R/T. The primers KC120 and KC121 were used to amplify 1205 bp *TRP1* gene and cloned into pJET1.2/blunt cloning vector. Plasmid pUC19 was used as a primary vector for plasmid constructs. 1.2 kb *TRP1* gene was cloned in BamHI- SalI site, and 591bp BamHI-SacI upstream fragment was cloned in the BamHI-SacI site of pUC19. SphI-SalI 506 bp downstream fragment was cloned in the above construct in SphI-SalI site. The cassette was released by digesting with SacI and transformed into yeast strain B-8728 containing a copy of *CCT7* in pRS316 plasmid. Gene deletion was done using the homologous gene disruption method. The primers KC316/ KC317 were used for internal amplification and KC542/KC129 were used for junction checking to verify the gene deletion. A point mutation was created from GGG to EGG of *CCT7* using primers KC474/KC475 with *CCT7* cloned in BamHI-SalI site of pRS315 using site-directed mutagenesis kit. For the aggregation visualization, the primers KC589/KC590 were used to amplify the *HSP104* gene (3181 bp, promoter and 3' end forming sequences) and cloned in BamHI-XhoI site of pRS11326. Subsequently, a DNA fragment (750bp) containing GFP was cloned at BamHI site to generate the plasmid pKA844. The GFP-tagged cassette was transformed in wild-type and mutant yeast (Sambrook and Russell 2001). The lithium acetate/ polyethylene glycol method was used to transform yeast cells (Hinnen et al. 1978). All the strains, plasmid constructs and primers used in the study are listed in Supplementary Table 1, 2, and 3.

2.3 Atomic Adsorption Spectroscopy:

Fresh yeast cells were inoculated in 20ml of YPD, grown till the early log phase. 1mM $CdCl_2$was added to it and grown for 16 hours at 30^oC, initial pH 6. Conditions were altered accordingly to study the effect of contact time and pH. The culture was centrifuged at 5000 rpm for 5 minutes, and the supernatant was analyzed for residual cadmium by Perkin Elmer AAS, PinAAcle 900F. The Q, uptake capacity (µg mg^{-1}) and E, removal efficiency (%) was calculated by

$$Q = \frac{(Ci - Ce)}{M} * V \quad (1)$$

$$E = \frac{(Ci - Ce)}{Ci} * 100 \quad (2)$$

Where Ci (µg ml^{-1}) is the initial concentration, Ce (µg ml^{-1}) is the final concentration of cadmium, M (mg) is the dry weight of yeast, and V (ml) is the volume (Perez-Marin et al. 2007).

2.4 Microscopic methods

Strains were grown till the early-log phase then 1mM $CdCl_2$ was added and grown for 4hours with and without cadmium. Cells were collected and washed with distilled water. Slides were prepared in 1% agar and seen under the Nikon ECLIPSE T*i*-Efluorescent microscope. For electron microscopy, cells were spread over 1% agar, layered the coverslip, and desiccated. These were then sputtered with gold particles for 15s and imaged using scanning electron microscope Hitachi SU6600 (Japan). 5µl of 2mg neutral red ml^{-1} was added to 25µl of cell culture and incubated for 5 minutes to visualize vacuoles, and slides were seen under the optical microscope (Corbacho el al 2010).

2.5 RNA preparation and real-time PCR

Total RNA isolation was done using the hot acid-phenol method as described. Eppendorf NanoDrop spectrophotometer was used for estimation of RNA concentration. DNaseI treatment was given to remove any DNA contamination in RNA samples and verified with standard PCR. cDNA from RNA samples were prepared using Thermo Fisher Scientific RevertAid first strand cDNA synthesis kit. Real-time quantitative PCR was performed using Bio-Rad CFX96 Real-time system in 20µl reactions taking 25ng cDNA $µl^{-1}$ in each sample using Thermo Fisher Scientific Maxima SYBR Green/ROX qPCR Master Mix. The in-built Bio-Rad system protocol (CFX_2 step ampl protocol) was used for RT-qPCR with additional melt curves after the amplification. Briefly, denaturation was done at 95^{o}C for 3 minutes, followed by 40 cycles of 95^{o}C for 10 seconds and 55^{o}C for 30 seconds. After amplification, melt curves were run at 65^{o}C to 95^{o}C for 5 seconds at increment of 0.5^{o}C. The gene expression difference was calculated as fold change using the ΔΔCt method (Schmittgen and Livak 2008). Triplicates were performed in all the PCR reactions.

2.6 Bioinformatics methods and tools:

Peptide sequences of eight yeast CCTs were retrieved from the *Saccharomyces* Genome Database. Prime module (version 11.1) of Schrödinger, (Schrödinger, LLC, New York, NY, 2017) was used to predict three-dimensional structures. Template structures 5GW4_H was selected based on the percentage identity. Clustal omega was used for multiple sequence alignment of protein sequences. Web logo model for conserved motif was prepared using consurf (Ashkenazy et al. 2016; Sievers et al. 2011).

3. Results And Discussion

In haploid *Saccharomyces cerevisiae* strain B-8728, the *CCT7* gene present in the genome was deleted by homologous recombination, providing an extra copy of the gene in pRS316 plasmid (*CEN6 URA3*). The size of the deletion cassette used was 2.2 kb. The accurate deletion was confirmed using two sets of PCR primers to amplify the 5' and 3' junctions (Supplementary Fig. 1a.). One of the two primers used for junction was made from the marker sequence, and the other corresponds to the sequence outside the flanking sequences used for deletion cassette. The primer KC542/KC317 and KC129/KC316 were used to check upstream and downstream junctions, respectively. The expected size for upstream junction PCR product was 921bp and 850bp for the downstream junction (Supplementary Fig. 1a and 1b). The *cct7* deletion mutants were selected on plate containing 5-fluoroorotic acid (FOA). As *CCT7* is an essential gene, deletant mutant will not grow on FOA plate. The mutant version of *CCT7* was placed in the cell by plasmid shuffling in which wild type copy of *CCT7* in pRS316 (*CEN6 URA3*) was replaced by mutant *CCT7* (G412E) present in pRS315 (*CEN6 LEU2*).

3.1 Effect of mutation on growth

CCT mutants are reported to have growth defects in earlier works (Lin et al. 1997; Narayanan et al. 2016). G412E mutant in Cct7p subunit has visible growth retardation in complete media at optimum temperature (Fig. 1). Doubling time was 3.47+/-0.2 hours and 2.05+/-0.2 hours of mutant and wild type, respectively. Actin is obligate TriC/CCT substrate that plays a central role in cytokinesis. Cdh1p and Cdc20p are components of the mitotic checkpoint complex (MCC) and inactivation of this complex facilitates cells to move in anaphase. Inactivation of complex occurs with the disassembly of MCC by CCT (Kaisari et al. 2017; Llorca et al. 2000). Similarly, slow growth was seen in a strain carrying *cct7* mutation in the conserved GDGTT motif of ATP binding pocket (Amit et al. 2010). The yeast strain carrying mutant *cct7* was investigated in various stress conditions to assess its sensitivity. Cell growth was at par with optimum conditions at acidic to alkaline pH, oxidizing agent H_2O_2 and redox agent dithiothreitol (DTT) however lesser than wild type (Supplementary Fig. 2).

Metal ions bind to the thiol group of cysteine residue and affect cellular proteins. Metal ions have a propensity to produce reactive oxygen species that causes protein damage. Mutant viability was tested against different metal salts, namely zinc chloride, copper sulphate, cadmium chloride, arsenous acid, and sodium arsenate. Except for arsenous acid (III), no further growth differences were observed than wild-type strain. On the contrary to As^{3+}, cells were growing better than wild type in 1mM cadmium chloride (Fig. 2). As^{3+} inhibits CCT complex and tubulin, actin polymerization by binding to its monomer (Pan et al. 2010; Thorsen et al. 2009). Cadmium produces protein aggregates in yeast; Heat shock proteins (HSPs) are up-regulated in the presence of both As^{3+} and Cd^{2+} (Jacobson et al. 2017).

3.2 Adsorption of cadmium in the mutant.

Mutant is growing in Cd (II) better than the wild type; tolerance to the metal ion is either attributed to the out flux of metal ion or hyper accumulation. Cadmium uptake efficiency is 10.54µg cadmium mg^{-1} and 9.05µg cadmium mg^{-1} for mutant and wild type, respectively. Cells were grown for 16, 24, and 48 hours

to study the effect of contact time on cadmium adsorption of mutant. The removal capacity was 42.75%, 46.70%, and 65.17% for 16, 24, and 48 hours respectively. Mutant and wild type were grown in pH 4, 6, and 7 with 1mM $CdCl_2$. Mutant can grow better at acidic pH4 with a removal capacity of 48.97% compared to pH6 with 42.75% (Fig. 3). Cadmium removal capacity was favoured by acidic pH4 and 48 hours contact time.

3.3 Aggregation of the protein

The heat shock protein 104 (Hsp104) is a cytosolic protein that, on the incidence of protein aggregates, gets recruited on-site and stimulates Hsp70 to bind this complex and assists in clearance. To visualize protein aggregates, Hsp104 was tagged with GFP and expressed in both wild type and mutant. In wild type, Hsp104 was dispersed all over the cytosol while aggregates were present in the mutant. These aggregates may have a protective function against oxidative stress. The amyloid plaque has metal chelation and antioxidant properties at macromolecular metal levels (Baruch-Suchodolsky and Fischer 2008, 2009; Carija et al. 2017). The aggregate formation was seen in both wild type and mutant when grown in the presence of cadmium (Jacobson et al. 2017) (Fig. 4).

3.4 Vacuole sequestration of cadmium and altered cell morphology

The mutant's cell size was enlarged and is roughly double the size of the wild type (Fig. 5). Larger cell size can be due to prominent vacuoles in the cell (Chan and Marshall 2014). For visualization, wild type and mutant were then stained with vacuole dye neutral red (Corbacho et al. 2010), mutants were able to retain more stain compared to wild type (Fig. 6a). It is evident that mutant has more pronounced vacuoles and possibly assisting in withstanding cadmium. Mutant was sensitive to lactic acid. Lactic acid causes vacuole fragmentation (Suzuki et al. 2012) (Fig. 6b). Metal chelation and vacuole sequestration are often adopted strategies in metal tolerant strains. Ycf1p and Bpt1p are vacuole ABC transporters (Jacobson et al. 2017; Sharma et al. 2002). Glutathione interacts with metal ions to form complexes, and these pumps influx complexes to the vacuole. Expression of the *YCF1* and *BPT1* genes was enhanced by ten-fold and two-fold in the mutant, respectively. *RDN18-1* was taken as the reference gene (Fig. 7). Mutation leads to enhanced expression of the two genes supported by sensitivity to lactic acid and thus prepared mutants for detoxification of Cd^{2+}.

4. Conclusion

The chaperonin CCT complex is a central molecule that, along with translation machinery, HSPs and ubiquitin, tightly maintains cellular protein homeostasis. Loss of proper folding or degradation leads to disturbance in cell physiology, such as in neurodegenerative disorders. The Cct7p subunit of the CCT complex has exhibited sensitivity to G412E mutation. Cells were enlarged, has slow doubling time, and presence of protein aggregates. Surprisingly, the mutant was generally resistant to oxidative stress and was accumulating cadmium better than the wild type. An increase in the expression level of metal ion vacuolar transporters genes, *YCF1* and *BPT1*, in mutant suggests metal influx to vacuoles. This study

provides a cross-talk between protein folding and stress pathways. Further research is needed to understand how a mutation in CCT prepares the cell for oxidative stress and overexpression of vacuolar transporters.

Declarations

Acknowledgment

We are thankful to Dr. B. Das, Jadavpur University, Kolkata for providing basic *Saccharomyces* plasmid, Dr. P. J. Bhatt, IIT Bombay and Dr. F. Sherman for XL1 and B8728. We thank Dr. George K. Varghese, NIT, Calicut for permitting and Ms. Ashwini S. K. for helping out with AAS facility and Dr. Rathinaswamy K, NIT, Calicut and Mr. Sushobhan Mahanty to help with florescent microscopy, Mr. Dileep Pullepu for his inputs in manuscript writing.

Author contribution

MAK and AD conceived the study. AD performed the research; all authors were involved in analysis of the data. AD wrote and MAK revised and confirmed the manuscript.

Funding

This study was supported by council of scientific and Industrial Research (CSIR) grant (No: 37 (1571)/12/EMRII).

Conflict of interest

All authors declare that they have no conflict of interest.

References

1. Amit M, Weisberg S J, Nadler-Holly M, McCormack E A, Feldmesser E, Kaganovich D, Willison K R, Horovitz A (2010). Equivalent mutations in the eight subunits of the chaperonin CCT produce dramatically different cellular and gene expression phenotypes. J Mol Bio 401(3): 532-543.
2. Hinnen A, Hicks J B, Fink G R (1978). Transformation of yeast. Proc Natl Acad Sci U S A 75 (4): 1929-1933.
3. Ashkenazy H, Abadi S, Martz E, Chay O, Mayrose I, Pupko T, Ben-Tal N (2016). ConSurf 2016: an improved methodology to estimate and visualize evolutionary conservation in macromolecules. Nucleic Acids Res 44(W1): W344-W350.
4. Baruch-Suchodolsky R, Fischer B (2008). Soluble amyloid β1−28−Copper(I)/Copper(II)/Iron(II) complexes are potent antioxidants in cell-free systems. Biochemistry 47(30): 7796-7806.
5. Baruch-Suchodolsky R, Fischer B (2009). Aβ40, either soluble or aggregated, is a remarkably potent antioxidant in cell-free oxidative systems. Biochemistry 48(20): 4354-4370.

6. Carija A, Navarro S, de Groot N S, Ventura S (2017). Protein aggregation into insoluble deposits protects from oxidative stress. Redox Biol 12: 699-711.
7. Carmichael J, Chatellier J, Woolfson A, Milstein C, Fersht A R, Rubinsztein D C (2000). Bacterial and yeast chaperones reduce both aggregate formation and cell death in mammalian cell models of Huntington's disease. Proc Natl Acad Sci U S A 97(17): 9701-9705.
8. Chagoyen M, Carrascosa J L, Pazos F, Valpuesta J M (2014). Molecular determinants of the ATP hydrolysis asymmetry of the CCT chaperonin complex. Proteins 82(5): 703-707.
9. Chan Y H, Marshall W F (2014). Organelle size scaling of the budding yeast vacuole is tuned by membrane trafficking rates. Biophys J 106(9): 1986-1996.
10. Corbacho I, Teixidó F, Velázquez R, Hernández L M, Olivero I (2010). Yeast vacuole staining using quinacrine and neutral red. Microorganisms in Industry and Environment World Scientific 659-661.
11. Gestaut D, Limatola A, Joachimiak L, Frydman J (2019). The ATP-powered gymnastics of TRiC/CCT: an asymmetric protein folding machine with a symmetric origin story. Curr Opin Struct Biol 55: 50-58.
12. Jacobson T, Priya S, Sharma S K, Andersson S, Jakobsson S, Tanghe R, Ashouri A, Rauch S, Goloubinoff P, Christen P, Tamás M J (2017). Cadmium causes misfolding and aggregation of cytosolic proteins in yeast. Mol Cell Biol 37(17): e00490-00416.
13. Jin M, Han W, Liu C, Zang Y, Li J, Wang F, Wang Y, Cong Y (2019). An ensemble of cryo-EM structures of TRiC reveal its conformational landscape and subunit specificity. Proc Natl Acad Sci U S A 116(39): 19513-19522.
14. Kaisari S, Sitry-Shevah D, Miniowitz-Shemtov S, Teichner A, Hershko A (2017). Role of CCT chaperonin in the disassembly of mitotic checkpoint complexes. Proc Natl Acad Sci U S A 114(5): 956-961.
15. Lin P, Cardillo T S, Richard L M, Segel G B, Sherman F (1997). Analysis of mutationally altered forms of the Cct6 subunit of the chaperonin from Saccharomyces cerevisiae. Genetics 147(4): 1609-1633.
16. Llorca O, Martín-Benito J, Ritco-Vonsovici M, Grantham J, Hynes G M, Willison K R, Carrascosa J L, Valpuesta J M (2000). Eukaryotic chaperonin CCT stabilizes actin and tubulin folding intermediates in open quasi-native conformations. EMBO J 19(22): 5971-5979.
17. Mischley L K, Standish L J, Weiss N S, Padowski J M, Kavanagh T J, White C C, Rosenfeld M E (2016). Glutathione as a biomarker in Parkinson's disease: associations with aging and disease severity. Oxid Med Cell Longev 2016: 9409363
18. Nadler-Holly M, Breker M, Gruber R, Azia A, Gymrek M, Eisenstein M, Willison K R, Schuldiner M, Horovitz A (2012). Interactions of subunit CCT3 in the yeast chaperonin CCT/TRiC with Q/N-rich proteins revealed by high-throughput microscopy analysis. Proc Natl Acad Sci U S A 109(46): 18833.
19. Narayanan A, Pullepu D, Reddy P K, Uddin W, Kabir M A (2016). Defects in protein folding machinery affect cell wall integrity and reduce ethanol tolerance in S. cerevisiae. Curr Microbl 73(1): 38-45.
20. Pan X, Reissman S, Douglas N R, Huang Z, Yuan D S, Wang X, McCaffery JM, Frydman J, Boeke J D (2010). Trivalent arsenic inhibits the functions of chaperonin complex. Genetics 186(2): 725-734.

21. Pérez-Marín AB, Zapata VM, Ortuño JF, Aguilar M, Sáez J, Lloréns M. (2007). Removal of cadmium from aqueous solutions by adsorption onto orange waste. J Hazard Mater 139(1): 122-131.
22. Reissmann S, Joachimiak L A, Chen B, Meyer A S, Nguyen A, Frydman J. (2012). A gradient of ATP affinities generates an asymmetric power stroke driving the chaperonin TRIC/CCT folding cycle. Cell Rep 2(4): 866-877.
23. Sambrook J F, Russell D W (2001). Molecular cloning: A laboratory manual. Cold Spring Harbor Laboratory Press.
24. Schmittgen T D, Livak K J (2008). Analyzing real-time PCR data by the comparative C(T) method. Nat Protoc 3(6): 1101-1108.
25. Selley M L, Close D R, Stern S E (2002). The effect of increased concentrations of homocysteine on the concentration of (E)-4-hydroxy-2-nonenal in the plasma and cerebrospinal fluid of patients with Alzheimer's disease. Neurobiol Aging 23(3): 383-388.
26. Sharma K G, Mason D L, Liu G, Rea P A, Bachhawat A K, Michaelis S (2002). Localization, regulation, and substrate transport properties of Bpt1p, a Saccharomyces cerevisiae MRP-Type ABC Transporter. Eukaryot Cell 1(3): 391-400.
27. Sievers F, Wilm A, Dineen D, Gibson T J, Karplus K, Li W, Lopez R, McWilliam H, Remmert M, Söding J, Thompson JD, Higgins D G (2011). Fast, scalable generation of high-quality protein multiple sequence alignments using Clustal Omega. Mol Syst Biol 7(1): 539.
28. Sot B, Rubio-Muñoz A, Leal-Quintero A, Martínez-Sabando J, Marcilla M, Roodveldt C, Valpuesta J M (2017). The chaperonin CCT inhibits assembly of α-synuclein amyloid fibrils by a specific, conformation-dependent interaction. Sci Rep 7: 40859-40859.
29. Spiess C, Meyer A S, Reissmann S, Frydman J (2004). Mechanism of the eukaryotic chaperonin: protein folding in the chamber of secrets. Trend Cell Biol 14(11): 598-604. doi:10.1016/j.tcb.2004.09.015
30. Suzuki T, Sugiyama M, Wakazono K, Kaneko Y, Harashima S (2012). Lactic-acid stress causes vacuolar fragmentation and impairs intracellular amino-acid homeostasis in Saccharomyces cerevisiae. J Biosci Bioeng 113(4): 421-430.
31. Thorsen M, Perrone G G, Kristiansson E, Traini M, Ye T, Dawes I W, Nerman O, Tamás M J (2009). Genetic basis of arsenite and cadmium tolerance in Saccharomyces cerevisiae. BMC Genomics 10(1): 105.
32. Thulasiraman V, Yang C F, Frydman J (1999). In vivo newly translated polypeptides are sequestered in a protected folding environment. EMBO J 18(1): 85-95.
33. Ursic D, Sedbrook J C, Himmel K L, Culbertson M R (1994). The essential yeast Tcp1 protein affects actin and microtubules. Mol Biol Cell 5(10): 1065-1080.
34. Yam A Y, Xia Y, Lin H T J, Burlingame A, Gerstein M, Frydman J (2008). Defining the TRiC/CCT interactome links chaperonin function to stabilization of newly made proteins with complex topologies. Nat Struct Mol Biol 15(12): 1255-1262.

Figures

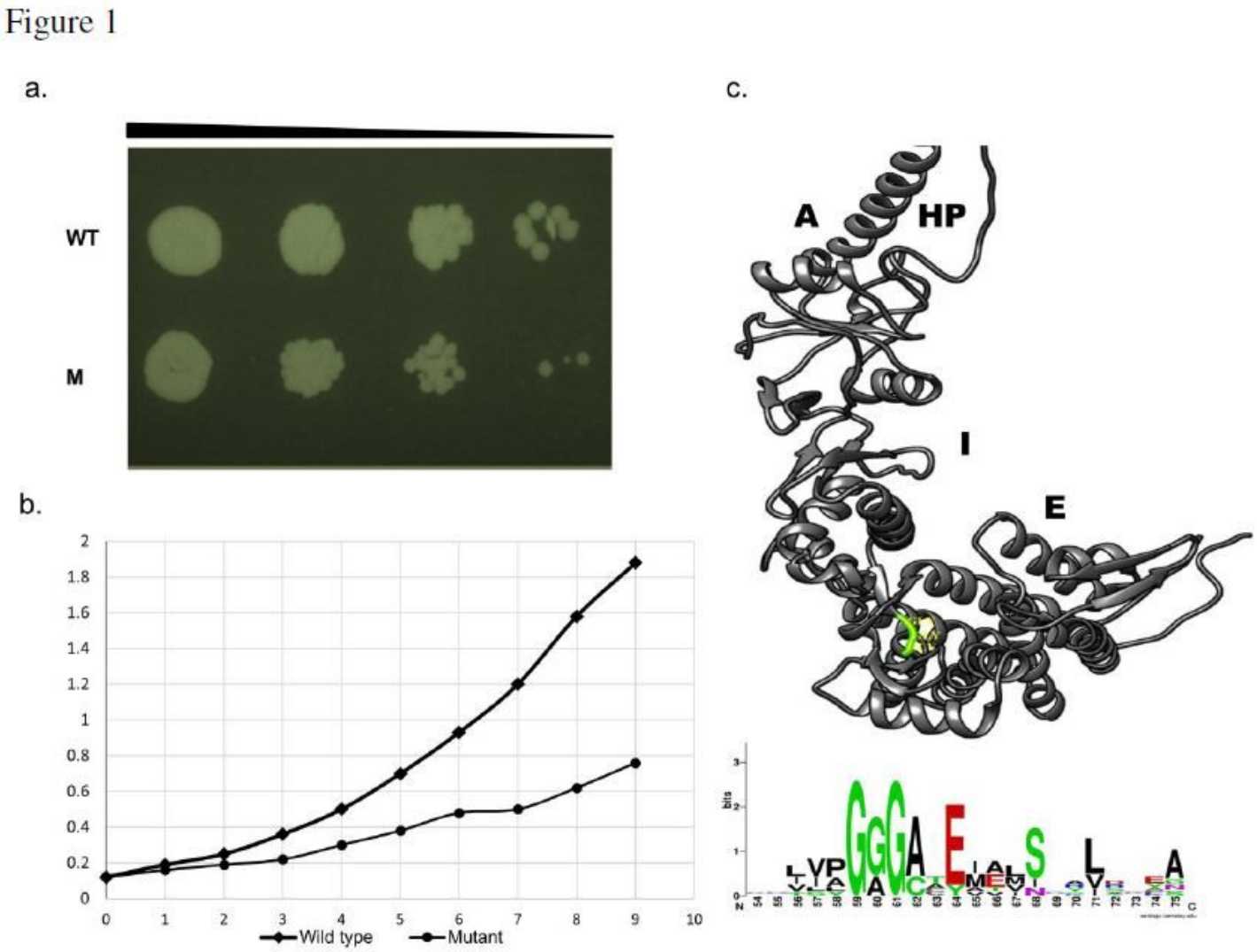

Figure 1

Growth assay: a. Spot assay of wild type and mutant on YPD plate at dilutions 104, 103, 102, and 101 CFU per spot as indicated. b. Liquid assay of wild type and mutant on YPD c. Modelling of Cct7p depicting location of conserved glycine residue at 412 position of equatorial domain and ConSurf model represents the conserved glycine residue in all eight subunits.

Figure2

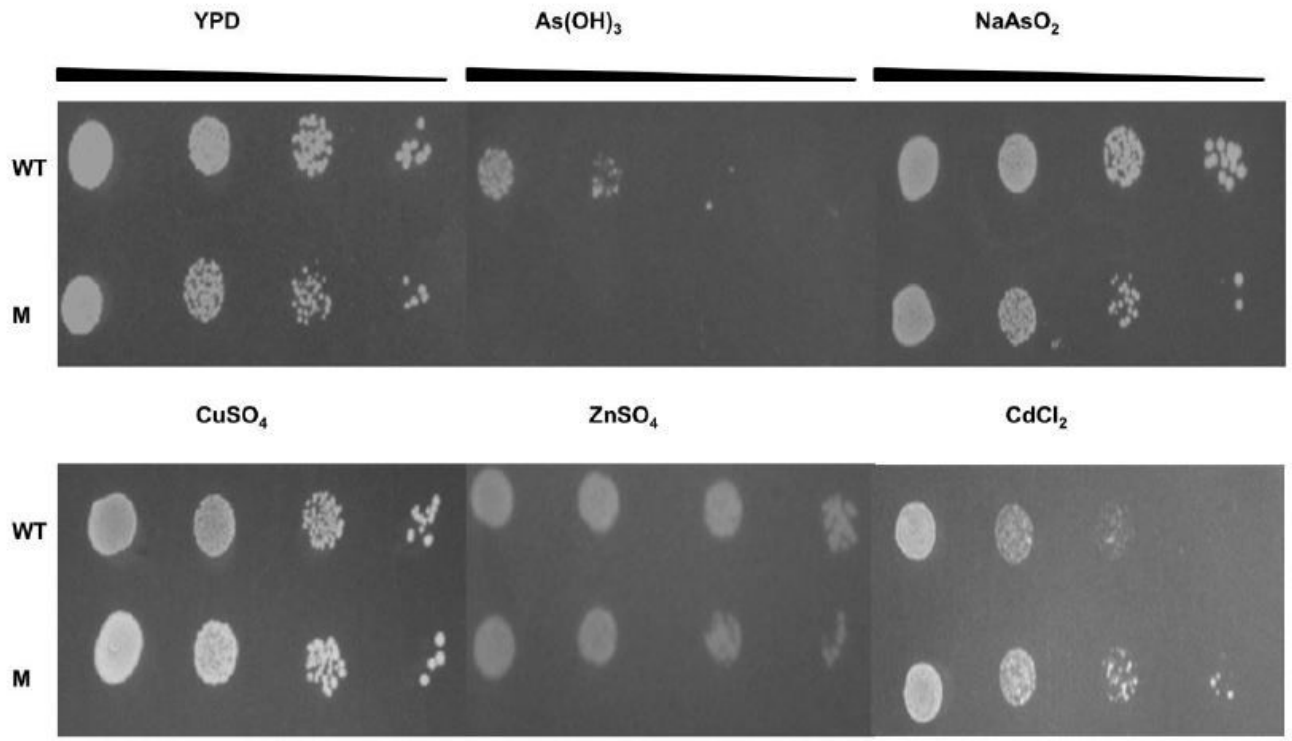

Figure 2

Spot assay of wild type and mutant on YPD plate containing 1mM of arsenous acid, 1mM of sodium arsenate, 2mM of copper sulphate, 2mM of zinc sulphate and 1mM of cadmium chloride at 30˚C at dilutions 104, 103, 102, and 101 CFU per spot as shown.

Figure 3

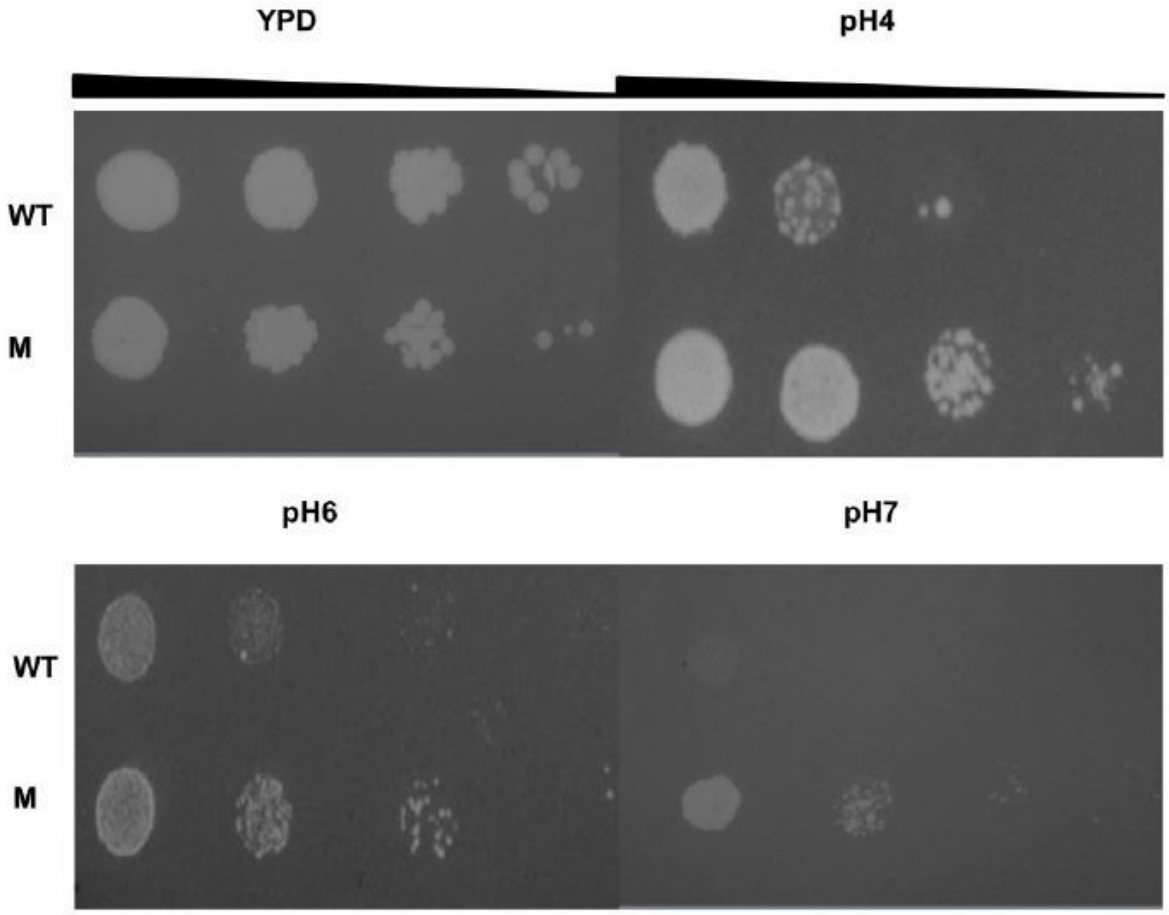

Figure 3

Spot assay wild type and mutant on YPD plates containing 1mM Cadmium chloride at 30˚C at pH4, 6 and 7 at dilutions 104, 103, 102, and 101 CFU per spot as indicated.

Figure 4

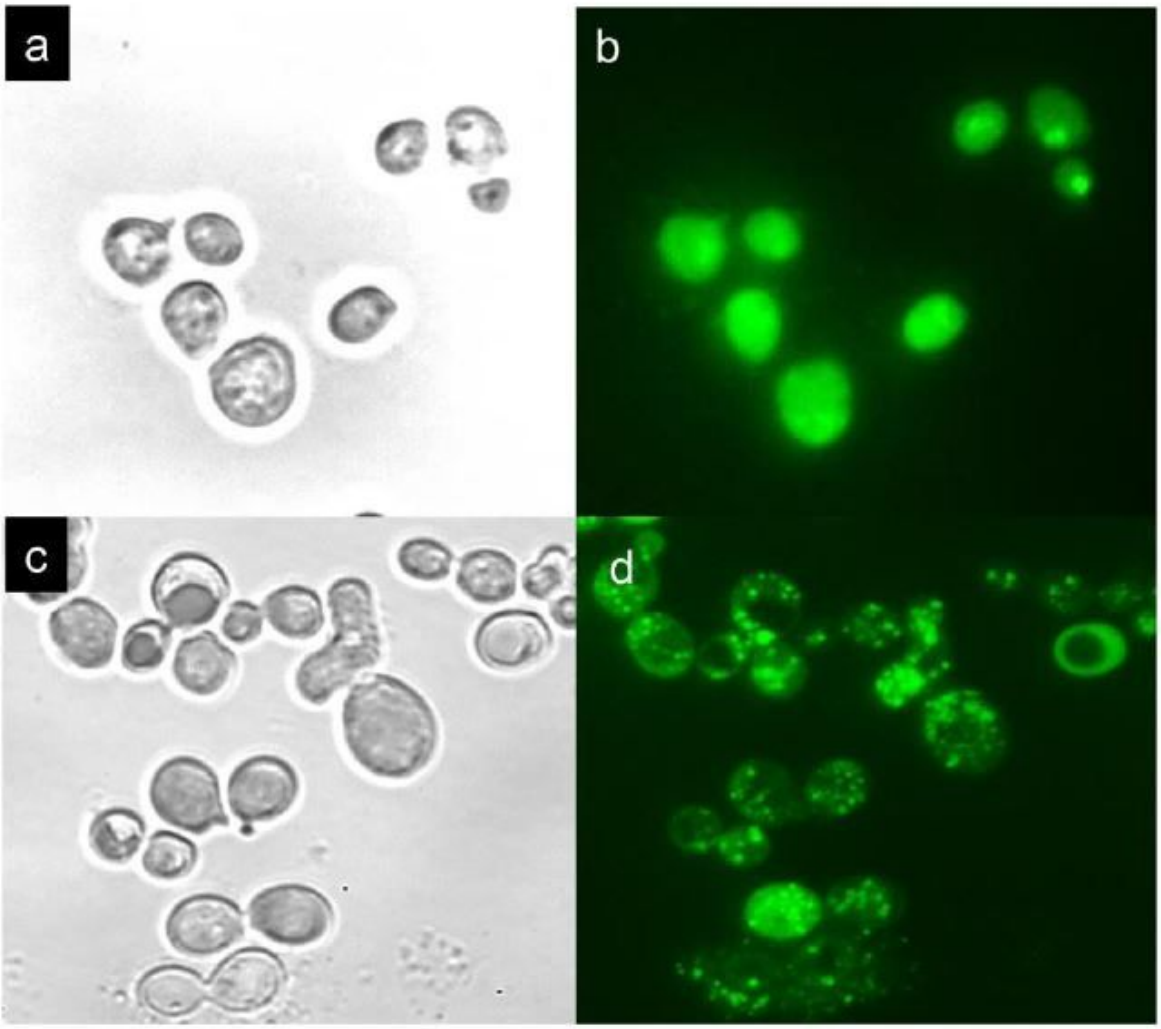

Figure 4

Florescent microscopy: Cells were transformed with plasmid containing HSP104 tagged with GFP to detect protein aggregates. a and b are wild type, c and d are mutants under bright field and FITC.

Figure 5

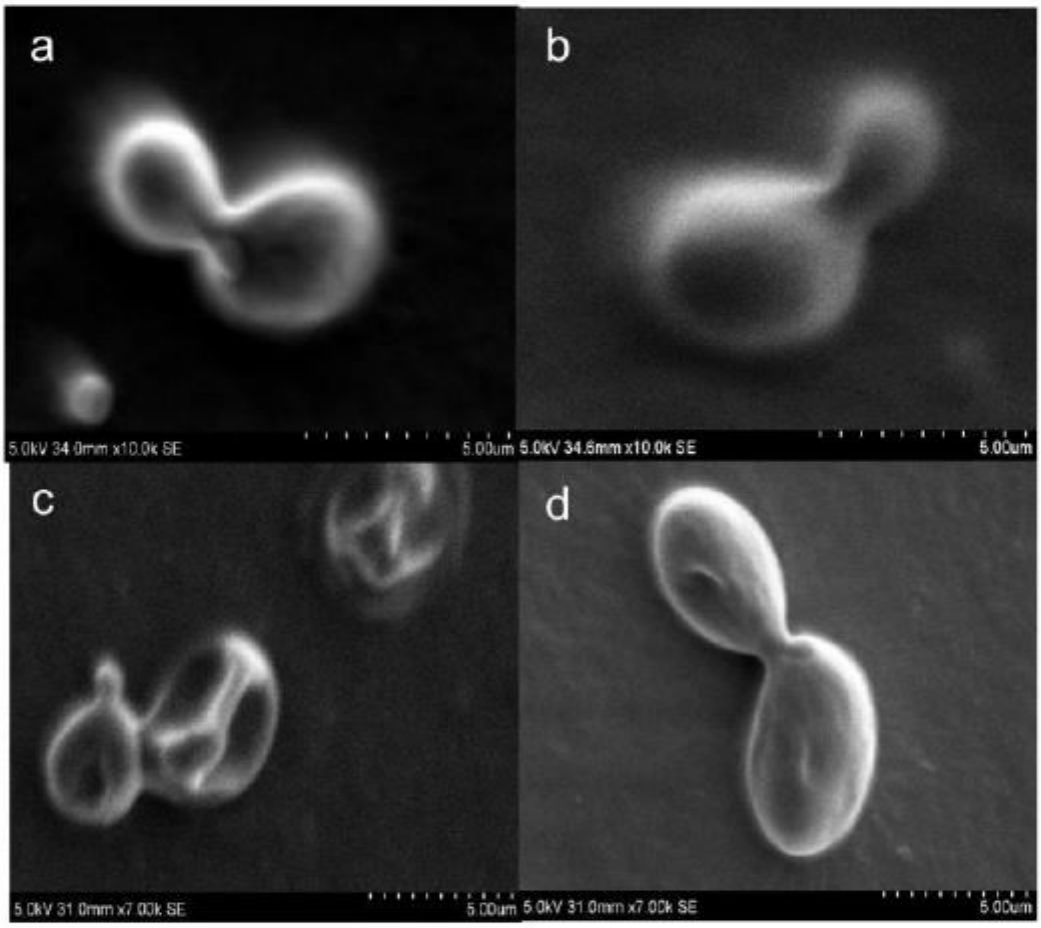

Figure 5

Scanning electron microscopy images of a. Wild type, b. Mutant c. Wild type treated with cadmium chloride and d. Mutant treated with cadmium chloride.

Figure 6

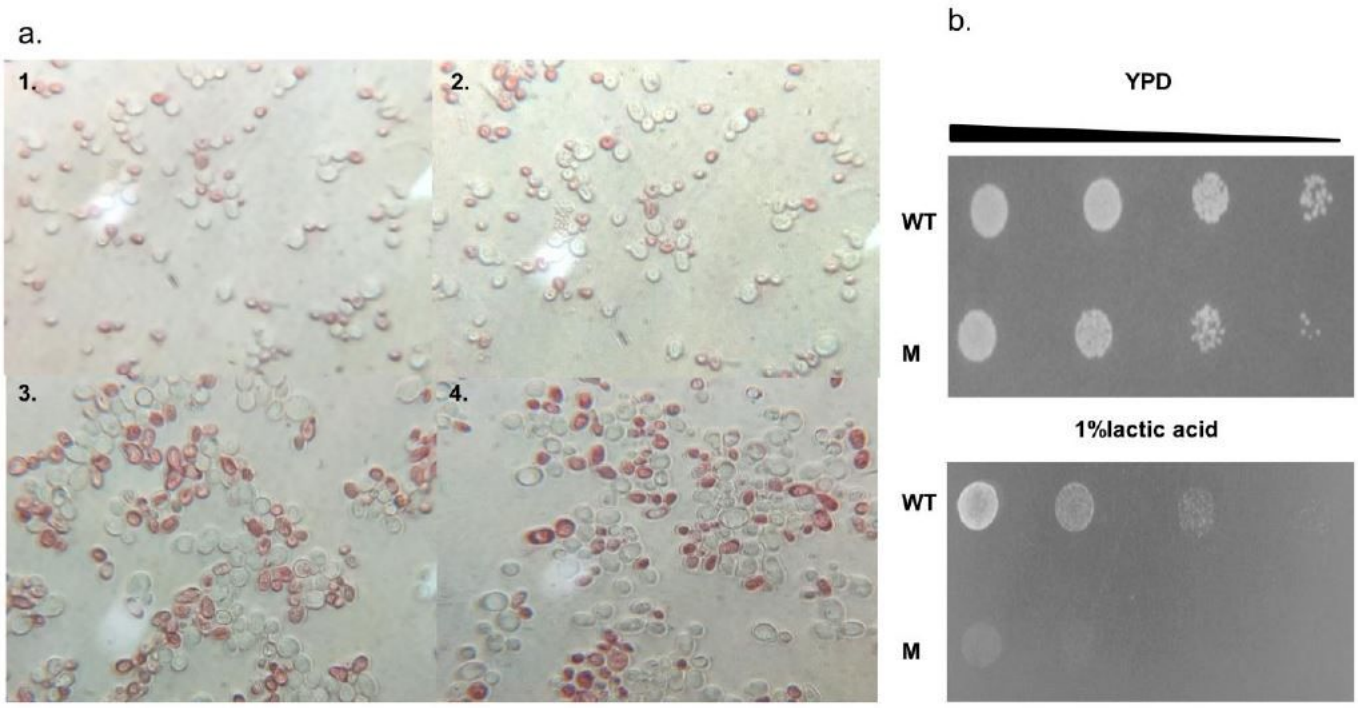

Figure 6

a. Microscopy images of wild type (1, 2) and mutant (3, 4) grown in YPD and YPD with cadmium chloride respectively stained with vacuole staining dye neutral red. b. Spot assay of parent strain B-8728, wild type and mutant on YPD plates containing 1% lactic acid at 30C as indicated.

Figure 7

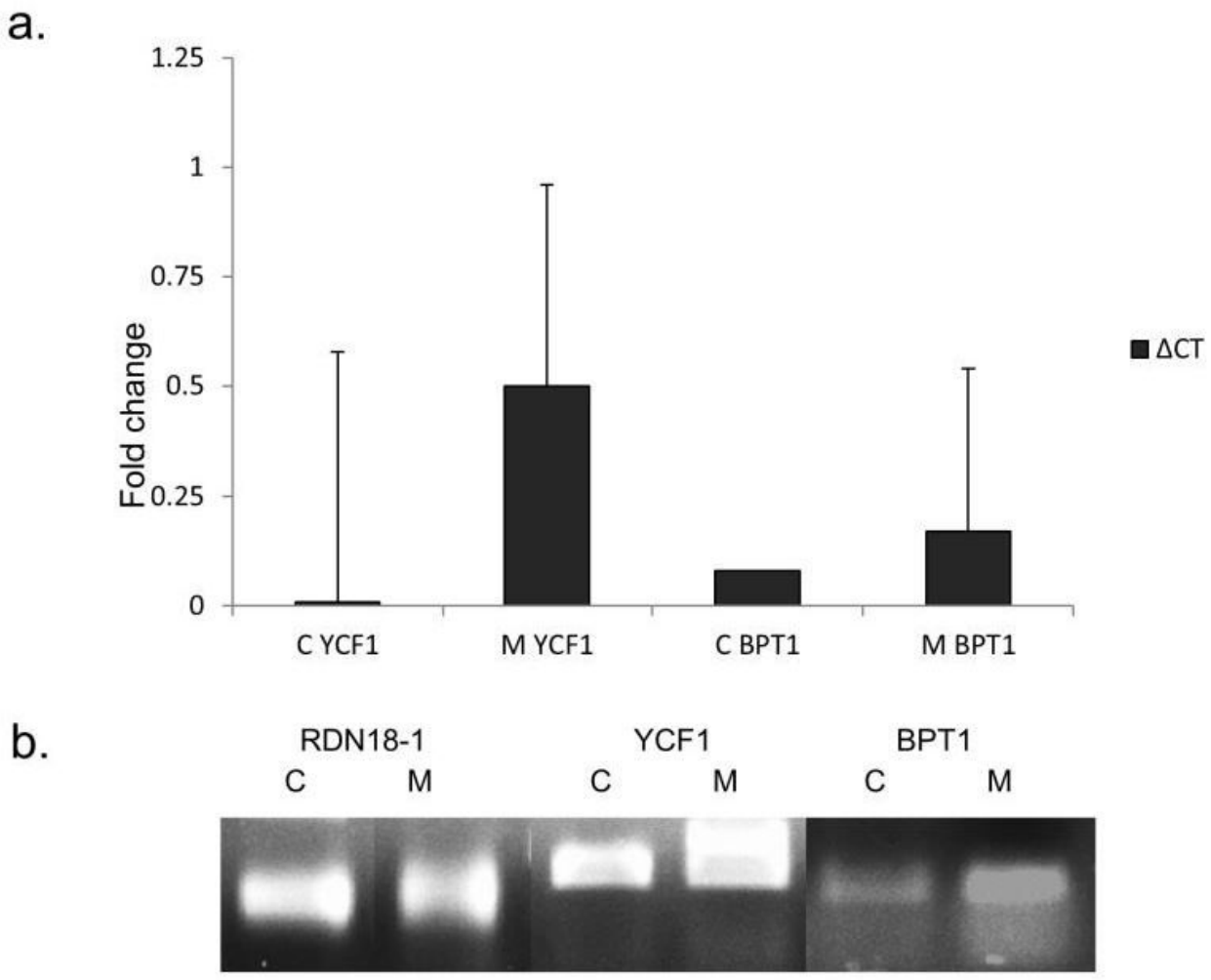

Figure 7

Real time PCR for vacuole pumps genes YCF1 and BPT1 in wild type and mutant a. Bar graph of ΔCT values of RT qPCR as depicted. b. Relative amplification for C-DNA of wild type and mutant was loaded in lane 1, 3, 5 and 2, 4, 6 respectively. Lane 1, 2; 3, 4 and 5, 6 contains reference gene RDN18-1, YCF1 and BPT1 respectively on 2% agarose gel.

Supplementary Files

This is a list of supplementary files associated with this preprint. Click to download.

- SupplementaryInformation.pdf